Available online at www.jbr-pub.org.cn

Open Access at PubMed Central

The Journal of Biomedical Research, 2021 35(6): 411–424

JBR

Original Article

Paclitaxel-induced stress granules increase *LINE-1* mRNA stability to promote drug resistance in breast cancer cells

Xiao Shi[1], Xinxin Si[1], Ershao Zhang[1], Ruochen Zang[1], Nan Yang[1], He Cheng[1,2], Zhihong Zhang[4], Beijing Pan[4], Yujie Sun[1,2,3,✉]

[1]*Key Laboratory of Human Functional Genomics of Jiangsu Province, Nanjing Medical University, Nanjing, Jiangsu 211166, China;*
[2]*Department of Cell Biology, School of Basic Medical Sciences, Nanjing Medical University, Nanjing, Jiangsu 211166, China;*
[3]*Collaborative Innovation Center for Cancer Personalized Medicine, Nanjing Medical University, Nanjing, Jiangsu 211166, China;*
[4]*Department of Pathology, the First Affiliated Hospital of Nanjing Medical University, Nanjing, Jiangsu 210036, China.*

Abstract

Abnormal expression of long interspersed element-1 (LINE-1) has been implicated in drug resistance, while our previous study showed that chemotherapy drug paclitaxel (PTX) increased LINE-1 level with unknown mechanism. Bioinformatics analysis suggested the regulation of *LINE-1* mRNA by drug-induced stress granules (SGs). This study aimed to explore whether and how SGs are involved in drug-induced LINE-1 increase and thereby promotes drug resistance of triple negative breast cancer (TNBC) cells. We demonstrated that SGs increased LINE-1 expression by recruiting and stabilizing *LINE-1* mRNA under drug stress, thereby adapting TNBC cells to chemotherapy drugs. Moreover, LINE-1 inhibitor efavirenz (EFV) could inhibit drug-induced SG to destabilize LINE-1. Our study provides the first evidence of the regulation of LINE-1 by SGs that could be an important survival mechanism for cancer cells exposed to chemotherapy drugs. The findings provide a useful clue for developing new chemotherapeutic strategies against TNBCs.

Keywords: LINE-1, stress granules, RNA stability, neoplasm drug resistance, triple negative breast cancer

Introduction

Triple negative breast cancers (TNBCs) are characterized by a lack of expression of the estrogen receptor (ER), progesterone receptor (PR), and human epidermal growth factor receptor 2 (HER2) and show high metastases and poor prognosis. Endocrine therapy and HER2 targeted therapies are usually ineffectual for TNBC patients because of high intratumor heterogeneity and a lack of molecular targets[1]. Chemotherapy is still the standard and main strategy for TNBC patients. However, 40%–80% of

✉Corresponding author: Yujie Sun, Key Laboratory of Human Functional Genomics of Jiangsu Province, Nanjing Medical University; and Department of Cell Biology, School of Basic Medical Sciences, Nanjing Medical University, 101 Longmian Avenue, Jiangning District, Nanjing Jiangsu 211166, China. Tel: +86-25-86869428, E-mail: yujiesun@njmu.edu.cn.

Received: 30 June 2021; Revised: 20 August 2021; Accepted: 24 August 2021; Published online: 30 October 2021

CLC number: R737.9, Document code: A

The authors reported no conflict of interests.

https://doi.org/10.7555/JBR.35.20210105

the patients develop chemotherapy resistance and have poor outcomes[2]. Elucidation of the molecular mechanisms underlying the drug resistance is essential for developing effective treatment strategies.

Long interspersed element 1 (LINE-1) is the only autonomously active retrotransposon in the human genome, and its total copy number accounts for approximately 20% of the genome[3]. An intact LINE-1 is about 6 kb in length and contain a 5′ untranslated region (UTR), two open reading frames (ORF1 and ORF2) that encode the ORF1p and ORF2p proteins, and a 3′UTR that ends in a polyadenosine-rich (poly (A)) tract. The ORF1p has RNA-binding and nucleic acid chaperon activities, whereas ORF2p has endonuclease and reverse transcriptase activities. LINE-1 expression is highly suppressed in normal differentiated somatic cells; however, in tumor cells, the expression of LINE-1 is abnormally activated, resulting in DNA double-stranded breaks, more homologous recombination and chromosome duplication through retrotransposition, which increase mutagenesis and genome instability[4]. Additionally, LINE-1 can also directly regulate gene expression and drug response *via* its RNA and protein[5–7]. Increased LINE-1 expression promotes cancer cell proliferation and alters the response of cancer cells to chemotherapy agents[8]. For example, LINE-1 ORF-1p can function as co-activator to promote the proliferation of breast cancer cells[9]. Inhibition of LINE-1 ORF1p enhances the response of hepatocellular carcinoma cells to epirubicin (EPI) and cisplatin (DDP)[10]. Notably, environmental stresses like chemotherapy agents, UV light and gamma radiation, can cause abnormal activation of LINE-1 expression in different cell context[11–12], which benefits cell survival under various stresses. It is reported that cells exposed to carboplatin prolong their own survival by increasing the expression of LINE-1[13]. We previously found that paclitaxel (PTX), a first line chemotherapy drug for TNBCs, caused an abnormal increase in LINE-1 expression level that significantly reduced the cell response to drugs. However, the mechanisms underlying drug-induced LINE-1 expression and subsequent chemotherapy resistance are unclear.

Stress granules (SGs) are assemblies of mRNAs and proteins that form in response to stressors like nutrient deprivation, heat, oxidative stress, and genotoxic stress. Their formation and dynamics significantly affect mRNA localization, translation, and stabilization, as well as the signaling pathways and stress responses of cells[14]. SGs favor cell survival during stress, while impairment of SG formation results in cell death. Importantly, several approved chemotherapeutic compounds have been reported to induce canonical or non-canonical SGs and thereby compromise treatment and promote drug tolerance[15–17]. SGs induce chemotherapy resistance by inhibiting pro-apoptotic signaling pathways, like the mTOR and MAPK pathways[18–19] or by increasing the stability of the mRNA of anti-apoptosis genes. For example, SGs formed in HeLa cells under the stress of bortezomib can stabilize the mRNA of p21, enhance the anti-apoptotic ability of cells, and develop bortezomib resistance in HeLa cells[20]. Several reports have suggested an association of LINE-1 and SGs. For example, Doucet *et al* have demonstrated that LINE- 1 ribonucleoprotein complexes (RNPs), including the ORF1p component, co-localize with the SG marker G3BP1 and other SG proteins[21]. This indicates that the mRNA of LINE-1 is able to localize within SGs. A SG transcriptome study provided that mRNAs with an overall length of the coding region longer than 2.5 kb and with longer untranslated regions (UTRs) were accumulated and enriched in the SGs[22]. The *LINE-1* mRNA, with a coding region of nearly 5 kb and a 1 kb 5′UTR, falls into this category. Our bioinformatics analysis using catRAPID and RPISeq website also predicted a strong interaction between *LINE-1* mRNA and T-cell intracellular antigen protein-1 (TIA1) and G3BP stress granule assembly factor 1 (G3BP1), two important SG marker proteins. This evidence suggested that *LINE-1* mRNA may be translocated to SGs during drug stress.

Based on these previous studies, we proposed that the formation of SGs induced by PTX could reduce the drug response of cancer cells by stabilizing *LINE-1* mRNA. We tested this hypothesis by systematic experiments using a PTX-resistant TNBC cell line and a xenograft mouse model. Our results demonstrated that SG formation was significantly increased in TNBC cells under PTX stress. Furthermore, drug-induced SGs recruited *LINE-1* mRNA, resulting in increased stability of the *LINE-1* mRNA and chemotherapy resistance in TNBC cells.

Materials and methods

Cell culture and reagents

The human TNBC cell line MDA-MB-231 was obtained from ATCC. The PTX-resistant cell line MDA-MB-231R and its parental MDA-MB-231S line was established by pulse selection with 100 nmol/L PTX, as described previously[23]. The human TNBC cell line MDA-MB-468 was kindly provided by Nan Qiao (SuZhou Institute of Systems Medicine, China).

LINE-1 expression plasmids PB015 and the vector plasmid PB001 with Neo resistance gene were gifts from Pasano Bojang Jr which was constructed by cloning LINE-1 sequence into a modified pGL4.15Luc2P vector[24]. We established stable LINE-1 overexpressing clones by transfecting PB015 into MDA-MB-231 cells, followed by G418 selection. The cells stably expressing LINE-1-Neo survived. A limiting dilution assay was then used to obtain a single cell incubated with conditioned medium until it grew into a clone. Clones transfected with PB001 as the control clone were named Ctr-clone. Two LINE-1 stable expressed clones named L1-clone 1 and L1-clone 2 were used for the experiments. All cells were maintained in L15 culture medium supplemented with 10% newborn calf serum, insulin (0.2 U/mL), 100 U/mL penicillin, and 100 U/mL streptomycin. All the cell lines were incubated at 37 °C in a humidified 5% CO_2 atmosphere. The following antibodies were used: antibody against LINE-1 (1:1000 dilution; Santa Cruz Biotechnology, USA) is a rabbit polyclonal antibody raised against amino acids 1081 to 1190 mapping near the C-terminus of human LINE-1 ORF2p; anti-ORF1p is a mouse monoclonal targets the sequence corresponding to 10 amino acids from the N-terminal region of LINE-1 ORF1p (1:1000 dilution; MilliporeSigma, USA); anti-TIA1 is a rabbit polyclonal to TIA1 C-terminal (1:1000 dilution; Abcam, UK); anti-GAPDH (1:20 000 dilution; Bioworld, China); anti-β-actin (1:4000 dilution; MilliporeSigma). Actinomycin D was obtained from GlpBio (USA). Efavirenz was purchased from ApexBio (USA). Paclitaxel, epirubicin, and cisplatin were purchased from Jiangsu Cancer Hospital (Nanjing, China).

Plasmid construction and cell transfection

In order to construct TIA1 expression plasmids, the coding sequence of TIA1 was amplified by Phanta MAX Super-Fidelity (Vazyme, China). The amplified fragments were purified and inserted into *Hin*d Ⅲ and *Xho* Ⅰ-digested pCMV6-Entry vector. The interfere plasmids of TIA1 were obtained by inserting two different shRNA sequences into the PLKO.1 vector respectively. The two shRNA sequences targeting TIA1 were: 5′-CGATTTGGGAGGTAGTGAA-3′ and 5′-AAGCTCTAATTCTGCAACTCT-3′. All the plasmids were transfected by Lipofectamine3000 (Thermo Fisher scientific, USA).

RNA extraction, qRT-PCR and RNA stability assay

Total RNA was extracted using TRIzol reagent (Invitrogen, USA), according to the manufacturer's protocol. Before reverse transcription, a step of removing genomic DNA was performed to eliminate interference from genomic DNA. Then cDNA was prepared by reverse transcribing 500 ng of total RNA, according to the manufacturer's instructions (Vazyme, China). Real-time PCR was performed using SYBR Green I Master Mix (Takara, Japan) and 0.5 μmol/L primers and run on a Light Cycler 480 (Roche, Switzerland) with typical amplification parameters (95 °C for 10 minutes, followed by 40 cycles of 95 °C for 30 seconds and 60 °C for 1 minute). The relative RNA level was determined by comparing the △CT value of each gene normalized to *ACTB* or *RPLP0* for each reaction. All samples were run in at least two duplicates. For mRNA stability test, cells were treated with 2 μmol/L actinomycin D for 2, 4, or 6 hours after transfection or drug treatment. The total RNA was then extracted. After normalized to *RPLP0*, the group without actinomycin D treatment as initial RNA level. Primers for *TIA1* were: forward, 5′-CGAGATGCCC AAGACTCTATACG-3′; reverse, 5′-CCTTACCCAT TATCTTCCGTCCA-3′. Primers for *LINE-1* ORF1 were: forward, 5′- GAGCTACGGGAGGACATTCA-3′; reverse, 5′-CTTCCAGTTGATCGCATCGG-3′.

Cell viability assay

Cells were seeded at a density of 5000 cells per well in 96-well plates. On the following day, cells were treated with different drugs for another 48 hours. At the end of the culture, cell viability was measured using the MTT assay, as described previously[23]. Simply, cells were treated by MTT (5 mg/mL) for 4 hours. Then discarded the supernatant and add 200 μL dimethyl sulfoxide (DMSO) into each well. After a mixing step, the absorbance at 570 nm for each well was measured by a microplate spectrophotometer (Bio-Rad, USA). All assays were carried out three times independently in triplicate.

RNA-FISH and protein immunofluorescence

Three 5'FAM modified fluorescent probes targeting LINE-1 RNA were obtained from Genepharma (China). The positions of the three probes targeting the LINE-1 RNA sequence (5′ to 3′) were: 1160–1214, 2350–2404, 5565–5621, sequences of the probes were as follows: 5′-AGAAGTGCTTAAAGGAGCT GATGGAGCTGAAAACCAAGGCTCGAGAACTA CGTGA-3′; 5′-GCACCCAGATTCATAAAGCAAG TCCTCAGTGACCTACAAAGAGACTTAGACTCC C-3′; 5′-ATGCACACGTATGTTTATTGCGGCACT ATTCACAATAGCAAAGACTTGGAACCAACC-3′. RNA-FISH was conducted according to the manufacturer's instructions. Briefly, cells were washed

twice with PBS, 5 minutes each time and then fixed with 4% paraformaldehyde in PBS for 20 minutes at room temperature, followed by a 15 minutes permeabilization step in 0.5% Triton in PBS and 5 minutes in 0.1% Tween-20 in PBS. After two 5 minutes washes with PBS, 100 μL 2× buffer C was added to each well and the plates were placed in a 37 °C incubator for 30 minutes. Probes were denatured at 73 °C for 5 minutes, hybridized at a 2 μmol/L working concentration with cells in a 37 °C incubator overnight for 12 to 16 hours. On the next day, the samples were removed from the incubator, the probe mixture was aspirated, and the cells were washed once with 0.1% Tween-20, 2× Buffer C and 1× Buffer C. After blocking with 5% FBS in PBS for 1 hour, the samples were incubated at 4 °C overnight with an antibody against TIA1 (1:100). Alexa Fluor 555 donkey anti-Rabbit (Beyotime, China) was used as the secondary antibody (1:50) and incubated for 1.5 hours at room temperature. Nuclei were stained with DAPI (10 mg/mL) after washing. Images were obtained by fluorescence microscope (Olympus, Japan, FU1200). Image analysis was conducted with Image J software, V1.52a (https://imagej.nih.gov/ij/download.html).

Western blotting

Total cellular protein extracts were obtained by lysis cell in lysis buffer contained 50 mmol/L Tris-HCl, 150 mmol/L NaCl, 0.02% sodium azide, 100 ng/ml phenylmethylsulfonyl fluoride, 0.1% SDS, 1% NP-40, and complete proteinase inhibitor mixture) as described previously[23] and were separated on 10% SDS-polyacrylamide gel and transferred to PVDF membranes. After blocking in 5% skimmed milk for 1 hour, the membranes were incubated with a primary antibody overnight at 4 °C. The membranes were then washed 3 times for 10 minutes in Tris-buffered saline containing Tween-20 (TBST) and incubated with an HRP-conjugated secondary antibody (Jackson Immuno-Research, USA) for 1 hour at room temperature. After washing 3 times for 10 minutes in TBST, the membranes were developed with an ECL detection system (Bio-Rad). Image analysis was conducted with Image J software, V1.52a (https://imagej.nih.gov/ij/download.html).

Animal experiments

Female nude mice (BALB/c-null, three-weeks-old) were purchased from the Model Animal Research Center of Nanjing University (Nanjing, Jiangsu, China) and bred in special pathogen-free (SPF) condition. MDA-MB-231R cells (1×10^7) were subcutaneously injected into the left axilla. After the tumor diameter had reached about 5 mm, the mice were divided randomly into two groups. PTX (10 mg/kg), DMSO (4 mg/kg) or EFV (20 mg/kg) were injected every 3 days by tumor *in situ* injection. The body weight and tumor sizes were measured every week. Tumor volumes were calculated using the formula: volume=0.5×(length×width^2). After four weeks of treatment, mice were sacrificed and their tumors were removed, weighed, and photographed. This study was carried out in strict accordance with the guidelines for the care and use of laboratory animals of the National Institutes of Health. Our protocol was approved by the Committee on the Ethics of Animal Experiments of Nanjing Medical University.

Statistical analysis

All experiments were repeated three times. Statistical differences between means were determined by the Students' *t*-test or one-way ANOVA. Values are expressed as means±standard error of triplicate measurements. $P<0.05$ was considered statistically significant.

Results

PTX-induced LINE-1 expression reduced the sensitivity of cells to chemotherapy agents

Western blotting showed higher LINE-1 protein level in the PTX-resistant MDA-MB-231R cell line than in its parental MDA-MB-231S cell line (***Fig. 1A***). MDA-MB-231 cells were then treated with 100 nmol/L PTX for 48 or 72 hours, and harvested for qRT-PCR analysis. The PTX treatment caused a significant increase in the endogenous *LINE-1* mRNA level, which was 1.5 to 2 times higher than that in the control (***Fig. 1B***, left panel). A similar drug-increased LINE-1 level was also observed in the MDA-MB-468 cell line (***Fig. 1B***, right panel). However, PTX had no significant influence on LINE-1 promoter activity (***Supplementary Fig. 1A***, available online).

We then established clones stably overexpressing LINE-1. The *LINE-1* mRNA levels in two LINE-1 overexpressing clones (L1-clone 1 and L1-clone 2) were nearly ten times higher than those in the control clone (Ctr-clone) (***Supplementary Fig. 1B***, available online). The protein levels in L1-clone 1 and L1-clone 2 were also higher than those in the Ctr-clone (***Supplementary Fig. 1C***, available online). The clones were subsequently used for downstream examination of drug responses. MTT results showed that compared to Ctr-clone, L1-clone 1 and L1-clone 2 were less sensitive to three chemotherapy drugs, PTX,

EPI, and DDP (***Fig. 1C***). The half maximal inhibitory concentration (IC_{50}) values and the resistance index (RI) of L1-clone 1 and L1-clone 2 were also increased (***Table 1***).

The LINE-1 inhibitor efavirenz (EFV)[25] was then used to further confirm the function of drug increased LINE-1 in drug resistance. The mRNA and protein levels of LINE-1 were significantly inhibited by EFV in MDA-MB-231R cells (***Supplementary Fig. 1D*** and ***E***, available online). When combined with EFV, all three anticancer drugs significantly decreased cell viability and showed lower IC_{50} values than cells not treated with EFV (***Fig. 1D*** and ***Table 2***).

Inhibition of LINE-1 by EFV increased the PTX sensitivity of MDA-MB-231R xenograft tumors

We determined whether inhibition of LINE-1 by EFV sensitized the drug-resistant breast cancer cells to PTX *in vivo* using a xenograft tumor model. We transplanted 1×10^7 MDA-MB-231R cells into female nude mice. When the tumors reached approximately 5 mm in diameter, the mice were randomly divided into two groups: a paclitaxel treatment group (10 mg/kg PTX plus 4 mg/kg DMSO) and a group treated with a combination of paclitaxel and EFV (10 mg/kg PTX plus 20 mg/kg EFV). Each group of mice was injected with drugs every three days. After four weeks of treatment, the mice were sacrificed and their tumors were removed, weighed and photographed. As showed in ***Fig. 2A***, the tumors of the group given the combined treatment grew more slowly than the tumors of the group that received PTX alone. Consistently, the weight and size of the tumors were significantly decreased in the combined treatment group (***Fig. 2B*** and ***C***).

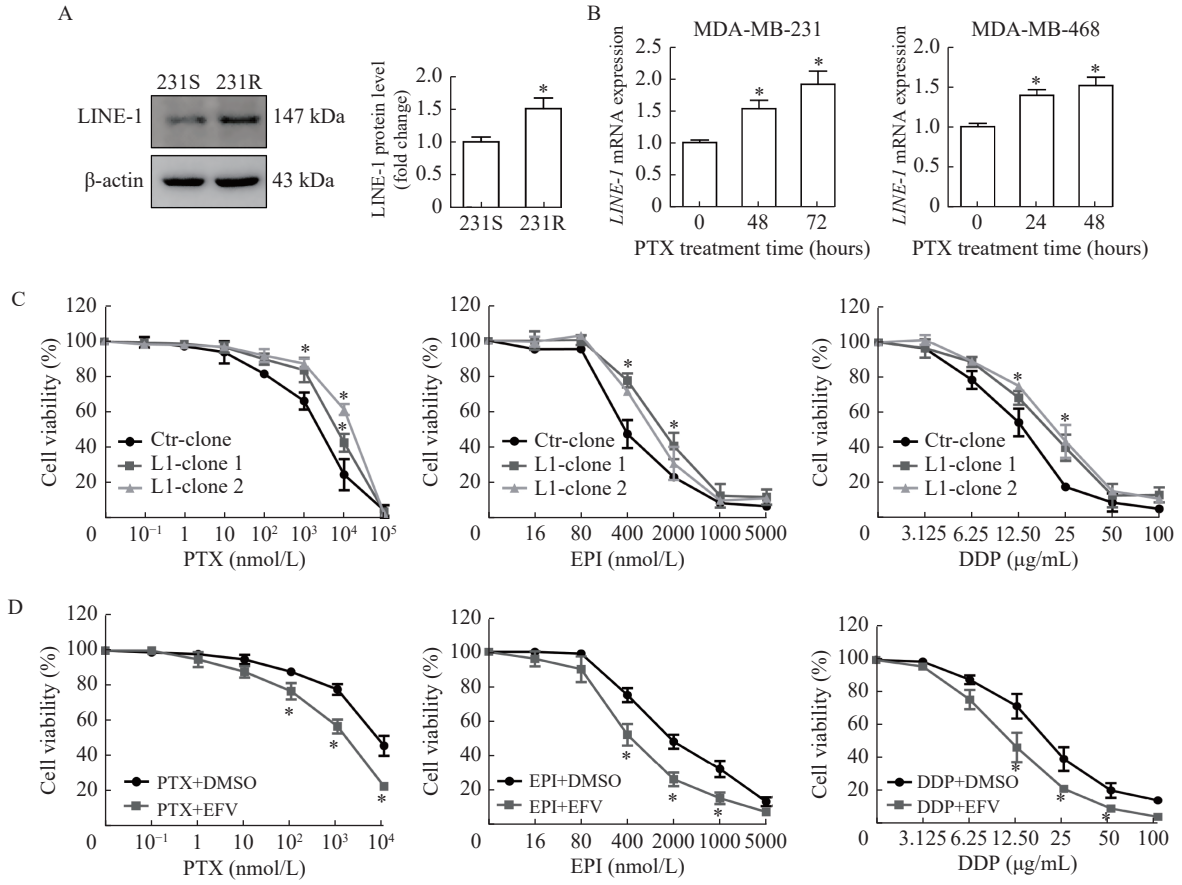

Fig. 1 **Paclitaxel-induced LINE-1 expression reduced the sensitivity of cells to chemotherapy agents.** A: Whole cell lysates were analyzed by Western blotting for LINE-1 protein levels in MDA-MB-231S and MDA-MB-231R cells. Antibody against ORF2p of LINE-1 was used to detect LINE-1. B: MDA-MB-231S cells were treated with 100 nmol/L PTX for 48 or 72 hours. MDA-MB-468 cells were treated with 50 nmol/L paclitaxel (PTX) for 24 or 48 hours. *LINE-1* mRNA level was normalized to *ACTB* mRNA level. C: LINE-1 overexpressing clones (L1-clone 1 and L1-clone 2) and control clone (Ctr-clone) cells were treated with an increasing concentration of PTX, epirubicin (EPI) or cisplatin (DDP) for 72 hours, and then cell viability was determined by the MTT assay. D: EFV reversed the PTX, EPI, and DDP resistance of MDA-MB-231R cells. MDA-MB-231R cells were treated with 45 μmol/L EFV or DMSO (vehicle control) in combination with increasing concentrations of PTX, EPI or DDP for 72 hours, as determined by cell viability assays. Mean values±SD (error bars) was shown for three independent experiments. Paired *t*-test was used to analyze the significance difference between the groups. $^*P<0.05$. DMSO: dimethyl sulfoxide.

PTX stress induced the formation of SGs and decreased sensitivity of TNBC cells to chemotherapy drugs

Immunofluorescence confirmed that PTX treatment induced the formation of SGs. Treatment of cells for 24 hours with 100 nmol/L PTX resulted in SG formation in approximately 40% of the cells (***Fig. 3A***) and was accompanied by a 2-fold increase in the protein level of TIA1 (***Supplementary Fig. 2A***, available online). PTX also induced SG formation in MDA-MB-468 cells, another TNBC cell line (***Supplementary Fig. 2B***, available online). The number of SG-positive cells following PTX treatment was decreased from 40% to 11% by interference with TIA1 (***Fig. 3B***). The interference efficiency of TIA1

Table 1 **The IC_{50} values of PTX, EPI, DDP in control and LINE-1 overexpression clones after 72 hours treatment with drugs**

Drugs	Clones	IC_{50}	RI
PTX (nmol/L)	Ctr-clone	1880.21±697.35	–
	L1-clone1	4438.80±739.13*	2.36
	L1-clone2	8034.46±779.624*	4.31
EPI (nmol/L)	Ctr-clone	429.14±116.63	–
	L1-clone1	1057.88±186.73*	2.47
	L1-clone2	739.50±156.96*	1.72
DDP (μg/mL)	Ctr-clone	13.22±2.41	–
	L1-clone1	17.26±3.41*	1.31
	L1-clone2	20.16±4.43*	1.53

Values are presented as means±SD. Statistics were performed by *t*-test. *P<0.05 *vs.* IC_{50} of Ctr-clone. PTX: paclitaxel; EPI: epirubicin; DDP: cisplatin; IC_{50}: half maximal inhibitory concentration; RI: resistance index.

Table 2 **IC_{50} values of PTX, EPI and DDP with or without EFV in MDA-MB-231R after 72 hours treatment**

Drugs	DMSO	EFV
PTX (nmol/L)	4041.29±895.14	777.15±91.50*
EPI (nmol/L)	2627.36±518.09	556.76±63.93*
DDP (μg/mL)	17.17±2.58	11.44±1.34*

Values are presented as mean±SD. Statistics were performed by *t*-test. *P<0 .05 *vs.* IC_{50} of DMSO. PTX: paclitaxel; EPI: epirubicin; DDP: cisplatin; DMSO: dimethyl sulfoxide; EFV: efavirenz; IC_{50}: half maximal inhibitory concentration.

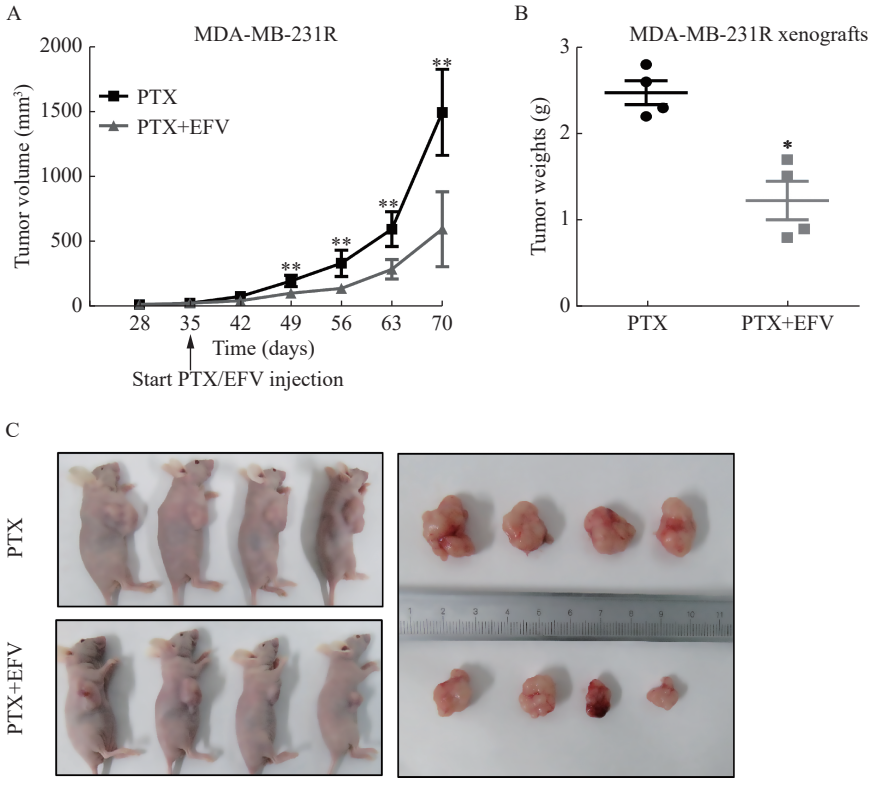

Fig. 2 **Inhibition of LINE-1 by EFV increased the sensitivity of MDA-MB-231R xenograft tumors to PTX.** Transplantation of 1×10^7 PTX-resistant MDA-MB-231R cells into the left armpit of female nude mice generated xenograft tumors. When the tumors were about 5 mm in diameter, the mice (n=4) were treated with PTX (10 mg/kg PTX plus 4 mg/kg DMSO) or a combination of PTX and EFV (10 mg/kg PTX plus 20 mg/kg EFV). A: Growth curves of the xenograft MDA-MB-231R tumors in nude mice calculated from the tumor volumes. Mean values±SD (error bars) was shown. **P<0.01, n=4. B: Average tumor weight after drug treatment. Mean values±SD (error bars) was shown. *P<0.05, n=4. C: Images of MDA-MB-231R xenograft tumors. Statistics were performed by one-way ANOVA. PTX: paclitaxel; EFV: efavirenz; DMSO: dimethyl sulfoxide.

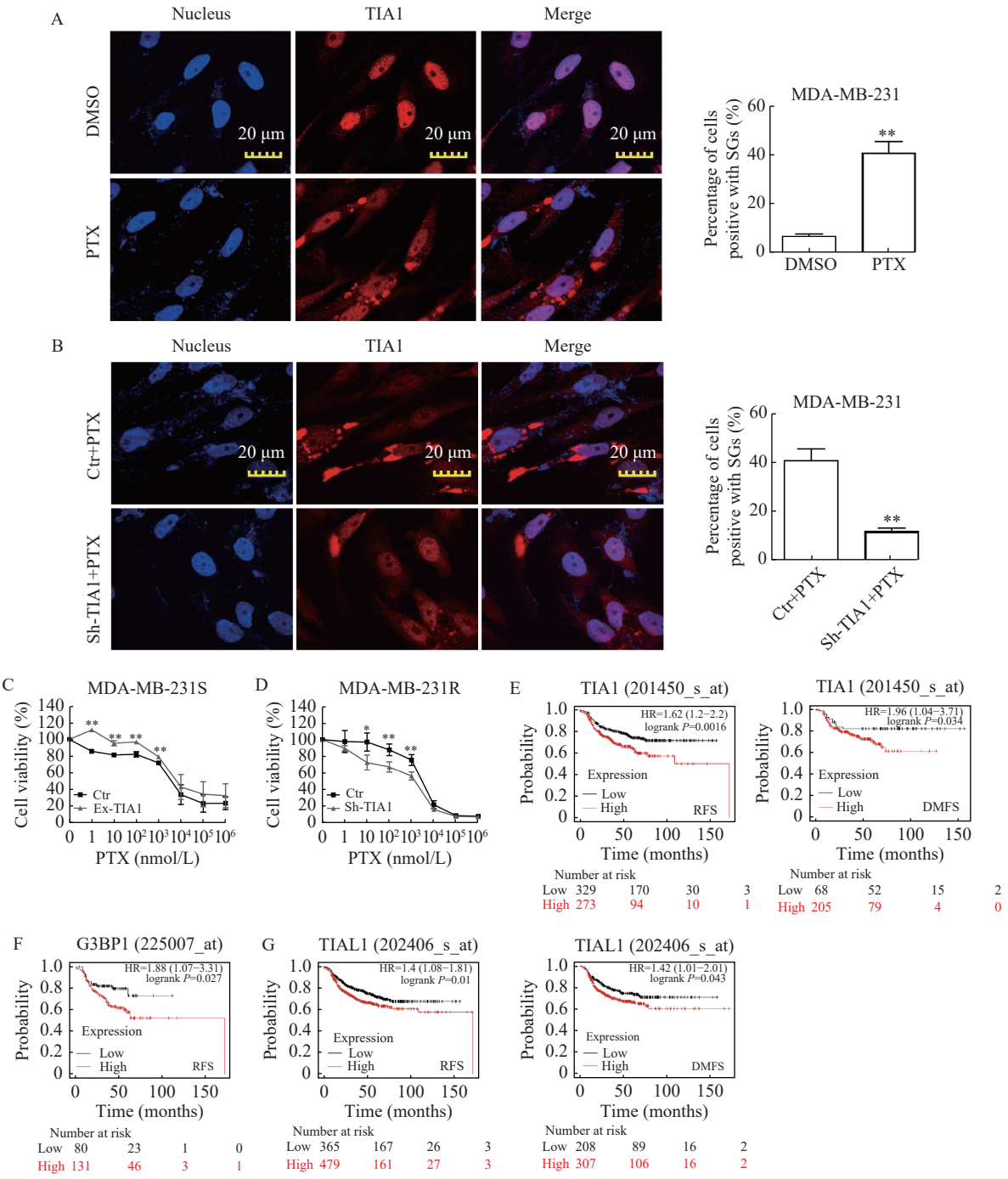

Fig. 3 **PTX-induced SGs decreased the sensitivity of TNBC cells to chemotherapy drug.** A: Representative images of SGs induced by a 24 hours treatment of MDA-MB-231 cells with 100 nmol/L PTX (left panel). The percentages of SG-positive cells were calculated (right panel). The yellow arrow points to SGs. Each independent experiment included an analysis of at least 50 cells per condition. B: MDA-MB-231 cells transfected with the TIA1 interference plasmid or a control plasmid, followed by 24 hours treatment with PTX. Immunofluorescence were then performed. The left panel is a representative image of the formed SGs, and the right panel is the calculated percentage of cells with SGs. C: Cell viability was tested after transfection of MDA-MB-231S cells with pCMV6-Entry vector (Ctr) or TIA1 expression plasmids (Ex-TIA1) and exposure to different concentrations of PTX for 72 hours. D: Viability of MDA-MB-231R cells was tested after 24 hours transfection with PLKO.1 vector (Ctr) or TIA1 interference plasmids (Sh-TIA1), followed by treatment with increasing concentrations of PTX for 72 hours. E: Kaplan-Meier analysis revealed a negative correlation between TIA1 and recurrence free survival (RFS, HR=1.62, P=0.0016, left panel) or distant metastasis-free survival (DMFS, HR=1.96 P=0.034, right panel) in breast cancer patients who had undergone chemotherapy but not endocrine therapy. F: A negative correlation between *G3BP1* mRNA level and RFS (HR=1.88, P=0.027). G: A negative correlation between *TIAL1* mRNA level and RFS (HR=1.4, P=0.01, left panel) or DMFS (HR=1.42, P=0.043, right panel). Mean values±SD (error bars) was shown for three independent experiments. Statistics were performed by t-test. $^{*}P<0.05$, $^{**}P<0.01$. PTX: paclitaxel; DMSO: dimethyl sulfoxide.

was shown in the ***Supplementary Fig. 2C*** (available online).

We also explored whether the PTX-induced SGs would cause breast cancer cells to develop chemotherapy resistance. MDA-MB-231S cells were transfected with TIA1 expression plasmids or vectors following 48 hours of PTX treatment and then harvested for cell viability test. MTT results showed TIA1 overexpression reduced the sensitivity of cells to PTX (***Fig. 3C***). The overexpression efficiency of TIA1 was shown in ***Supplementary Fig. 2D*** (available online). By contrast, interference with TIA1 expression sensitized PTX-resistant MDA-MB-231R cells to PTX (***Fig. 3D***). At last, we analyzed the relationship between expression level of SG marker protein TIA1, G3BP1, TIAL1 and clinical outcomes using a free online survival analysis tool Kaplan-Meier Plotter[26]. Our analysis included patients who received chemotherapy only, and excluded patients who received endocrine therapy, *etc*. As showed in ***Fig. 3E***, breast cancer patients with high TIA1 expression had worse recurrence free survival (RFS) and distant metastasis-free survival (DMFS). A negative correlation between RFS or DMFS with another two SG marker protein TIAL1 and G3BP1 was also obtained (***Fig. 3F*** and ***G***). These results indicated that the induction of SGs by chemotherapy drugs could reduce the subsequent responses of breast cancer cells to chemotherapy agents.

PTX-induced SGs recruited *LINE-1* mRNA in TNBC cells

The predictions from the catRAPID website[27] indicated that TIA1 had a strong interaction with LINE-1 5′UTR and a small affinity with its 3′UTR (***Supplementary Fig. 3***, available online). The predicted TIA1 binding region was mainly in the amino acids 111 to 162, corresponding to the RNA recognition motif 2 (RRM2) domain (its main RNA binding domain) (***Supplementary Table 1***, available online). The RPISeq website[28] predicted an interaction probability for LINE-1 RNA and TIA1 between 0.7 and 0.98. The interaction probability generated by RPISeq ranged from 0 to 1 and a probability >0.5 was considered positive. The prediction results for both websites indicated that TIA1 had a strong tendency to bind LINE-1 RNA. The RNA fluorescence *in situ* hybridization and protein immunofluorescence results showed that LINE-1 RNA was localized with TIA1, and that the average co-localization was significantly higher in the PTX-treated group (36.9%) than in the control group (9.6%). By contrast, TIA1 interference reduced the percentage of cells with LINE-1 RNA localized in SGs to 21.7% in PTX-treated cells (***Fig. 4A***). Consistently, a high TIA1 level led to the assembly of SGs as well as a strong localization of LINE-1 RNA within the SGs (***Fig. 4B***). These results indicated a recruitment of LINE-1 RNA to SGs under PTX stress.

PTX-induced SGs increased *LINE-1* mRNA stability and level

PTX treatment increased the half-life of *LINE-1* mRNA as well as the mRNA level (***Fig. 5A***). Overexpression of TIA1 also increased the stability and level of *LINE-1* mRNA (***Fig. 5B***), while TIA1 interference decreased the *LINE-1* mRNA stability following PTX exposure (***Fig. 5C***). The same reversal of PTX-enhanced *LINE-1* mRNA stability by TIA1 interference was observed in the MDA-MB-468 TNBC cell line (***Supplementary Fig. 4A*** and ***B***, available online). Moreover, interference of TIA1 partly inhibited the elevation of *LINE-1* mRNA level induced by PTX (***Fig. 5D***), indicating that PTX-induced SGs aid in stabilizing *LINE-1* mRNA during drug stress.

EFV reduced the stability of *LINE-1* mRNA by inhibiting the formation of SGs

EFV, an inhibitor of LINE-1, suppressed the increase in *LINE-1* mRNA expression induced by PTX. We testified whether EFV reduces the level of LINE-1 by inhibiting the formation of SGs under PTX stress. The proportion of cells containing SGs was 44% following treatment with PTX, but treatment with EFV in combination with PTX reduced this proportion to 6% (***Fig. 6A***), indicating that EFV treatment significantly inhibited the formation of SGs under PTX stress. RNA stability experiments further confirmed that EFV significantly reversed the stability of *LINE-1* mRNA increased by PTX (***Fig. 6B***), indicating that EFV can reduce the stability of *LINE-1* mRNA by inhibiting the PTX-induced formation of SGs.

Discussion

In the present study, we demonstrated that exposure of TNBC cells to the chemotherapy agent PTX could induce the formation of SGs and that SG formation enhanced drug resistance by stabilizing *LINE-1* mRNA. This work has therefore established a significant functional link between SGs, abnormal LINE-1 expression, and drug resistance. Our studies have several implications.

First, SGs are an important regulator of the *LINE-1* mRNA half-life during chemotherapy agent stress in

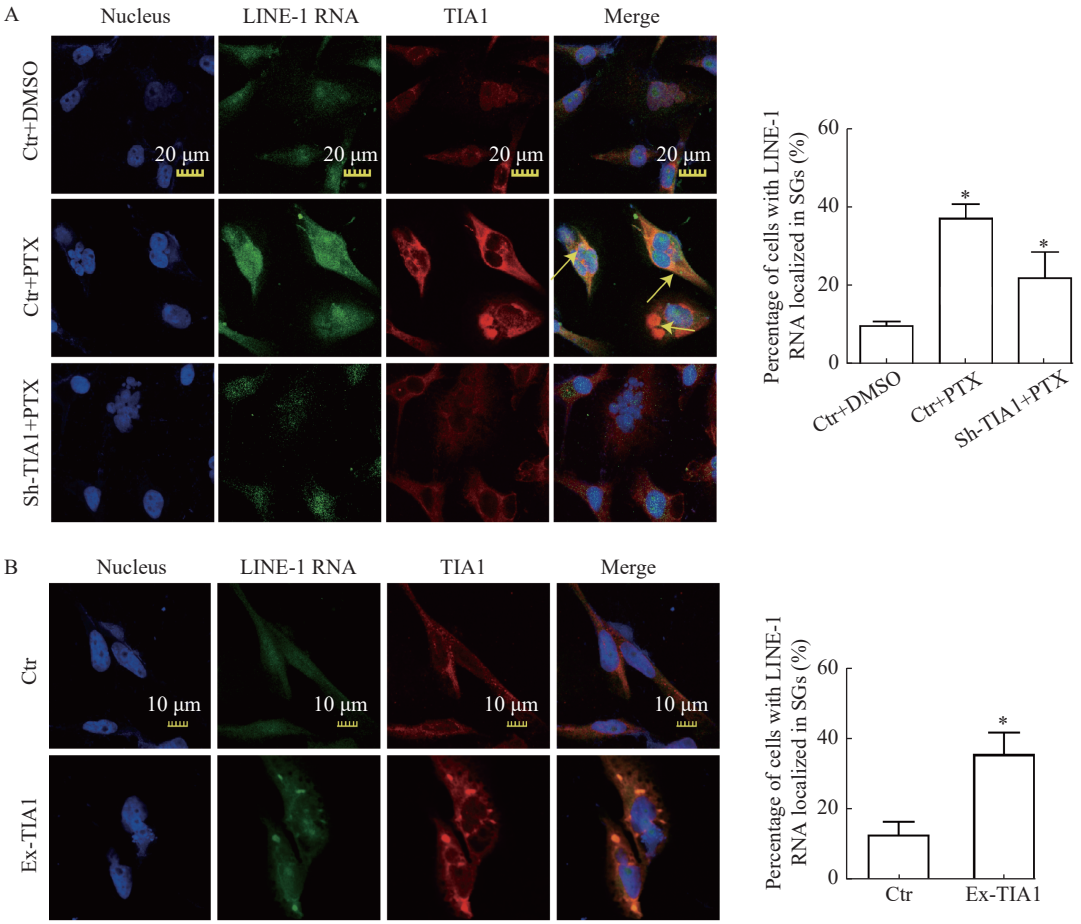

Fig. 4 **PTX-induced SGs recruit *LINE-1* mRNA in TNBC cells.** A: Representative images showing that LINE-1 RNA colocalized with SGs (left panel) and the calculated percentages of colocalization-positive cells (right panel). MDA-MB-231 cells were transfected with PLKO.1 vector (Ctr) or TIA1 interference plasmids (Sh-TIA1) for 24 hours, followed by 24 hours treatment with DMSO (vehicle control) or 100 nmol/L PTX. Colocalization of LINE-1 RNA with SGs was determined by immunofluorescence and RNA FISH. The yellow arrow points to the colocalization of LINE-1 RNA with SGs. B: Representative images showed significant colocalization of LINE-1 RNA with SGs in cells transfected with pCMV6-Entry vector (Ctr) or TIA1 overexpression plasmids (Ex-TIA1) (left panel). The percentages of colocalized cells were calculated (right panel). The yellow arrow points to the colocalization of LINE-1 RNA with SGs. Mean values±SD (error bars) was shown for three independent experiments. Each independent experiment included an analysis of at least 50 cells per condition. Statistics were performed by *t*-test. **P*<0.05. PTX: paclitaxel; DMSO: dimethyl sulfoxide.

TNBC cells. The expression of LINE-1 can be regulated at both the transcriptional and post-transcription levels in response to a variety of cellular environments[29–31]. RNA modifications or microRNAs were reported to regulate the half-life of *LINE-1* mRNA in cancer cells. For example, LINE-1 RNA stability is negatively regulated by TUT4/7-mediated 3'uridylation[32], whereas miR-128 directly binds to the 3′UTR of LINE-1 RNA to induce mRNA degradation and further decrease its expression and retrotransposition[33–34]. However, compared with the regulation of LINE-1 transcription in cancer cells, studies on the *LINE-1* mRNA half-life under chemotherapy stress are very limited. Here we demonstrated that SGs induced by the chemotherapy agent PTX could recruit *LINE-1* mRNA, thereby increasing the mRNA half-life and expression level (***Fig. 4A***, ***Fig. 5A***). The use of interference TIA1 or treatment with EFV to inhibit SG formation also reduced the stability of LINE-1 (***Fig. 3B***, ***Fig. 5C***, ***Fig. 6A*** and ***B***). These results identified SG as a new factor that regulates *LINE-1* mRNA stability under drug stress.

Two possibilities might explain how SGs regulate *LINE-1* mRNA stability. One is that mRNA stability is directly regulated by the TIA1 component. Some RNA binding proteins bind to the poly(A) tails of target RNA, and this may protect the proteins from undergoing uridylation and decay[32]. TIA1 is an RNA binding protein that has three RNA RRMs[35]. TIA1 also has binding sites in the LINE-1 RNA 3′ poly (A) tail (***Supplementary Fig. 3***), indicating that it is capable of binding LINE-1 RNA. In partial support of this, Meyer *et al* found that double knockout TIA1 and TIA1-like1 (TIAL1) decreased mRNA stability of

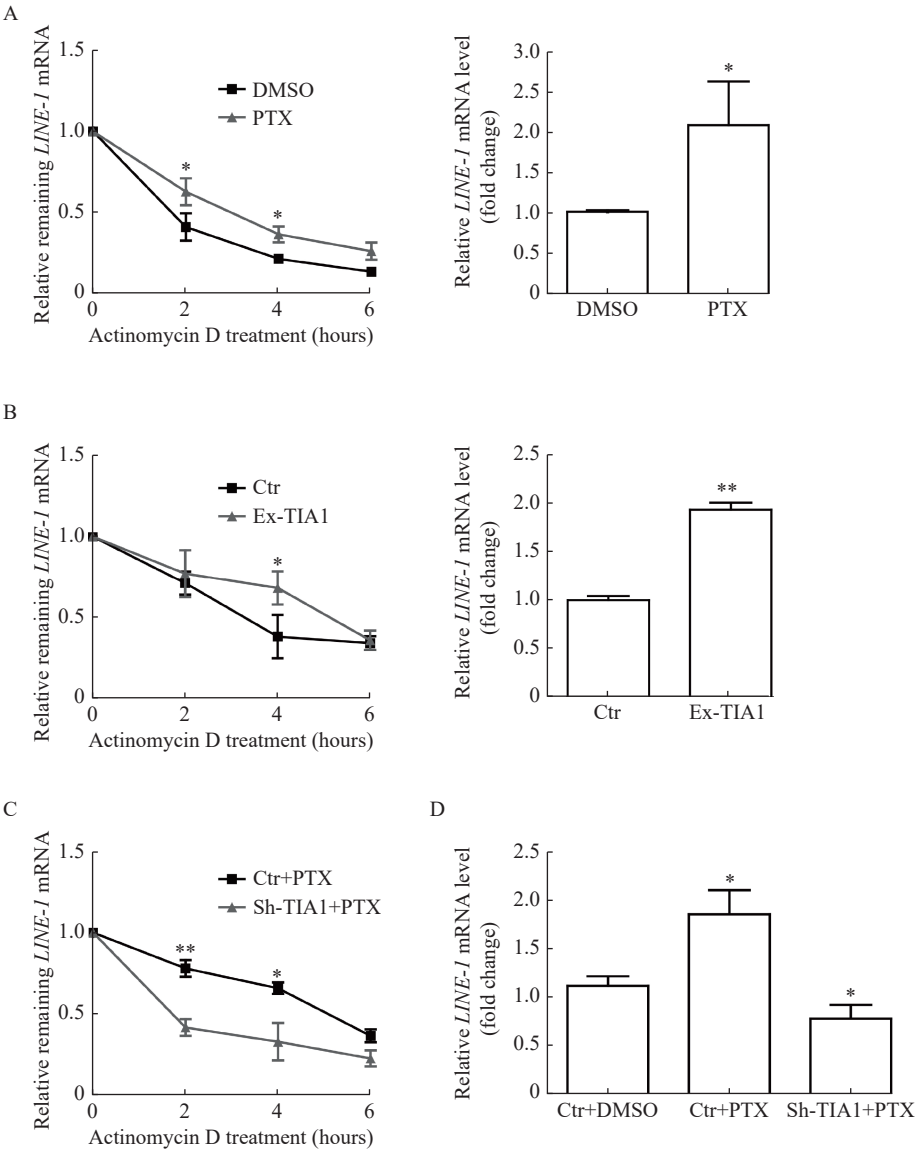

Fig. 5 **PTX-induced SGs increased *LINE-1* mRNA stability and level.** A: MDA-MB-231 cells were treated with DMSO or 100 nmol/L PTX for 48 hours, followed by 2, 4, or 6 hours treatment with 2 mol/L actinomycin D to inhibit transcription. qRT-PCR was used to analyze the decay of mRNAs (left panel). The relative level of *LINE-1* mRNA was calculated in cells without actinomycin D treatment (right panel). B: Cells were transfected with TIA1 overexpression (Ex-TIA1) or pCMV6-Entry (Ctr) plasmids for 24 hours, followed by transcription inhibition with 2, 4, or 6 hours treatment with 2 μmol/L actinomycin D. Total RNA was then extracted for qRT-PCR (normalized to *ACTB* mRNA levels). The left panel shows the relative stability of *LINE-1* mRNA; the right panel showed the level of *LINE-1* mRNA. C: Cells were transfected with PLKO.1 (Ctr) or TIA1 interference (Sh-TIA1) plasmids for 24 hours, followed by 48 hours exposure to PTX and then exposure to actinomycin D for different times. qRT-PCR was used to analyze the decay of mRNAs (normalized to *ACTB* mRNA levels). D: Cells were transfected with PLKO.1 (Ctr) or TIA1 interference plasmids for 24 hours and then treated with DMSO or 100 nmol/L PTX for another 48 hours. The relative mRNA levels of *LINE-1* were then measured by RT-PCT (normalized to *ACTB* mRNA levels). Mean values±SD (error bars) was shown for three independent experiments. Statistics were performed by *t*-test. $^{*}P<0.05$, $^{**}P<0.01$. PTX: paclitaxel; DMSO: dimethyl sulfoxide.

target genes that have TIA1 binding sites located in their 3′UTRs[36]. Another possibility is the stability of LINE-1 RNA is regulated by protective mRNPs formed in SGs. Bley *et al* pointed out that SGs recruited proteins and mRNAs to form protective messenger ribonucleoprotein complexes (mRNPs) that were indispensable in preventing mRNA degradation[37]. Our results confirmed the transport of LINE-1 RNA into SGs during PTX stress (***Fig. 4A***). The mRNA half-life of LINE-1 decreased after disruption of SG formation by interference TIA1 (***Fig. 3B*** and ***Fig. 5C***). Goodier *et al* found that the LINE-1 ORF1p colocalized with a known RNA stabilizer protein YB-1 in SG loci[38]. Since the LINE-1 protein has a *cis* preference for its RNA, a reasonable explanation is that LINE-1 RNA, in combination with YB-1, ORF1p, ORF2p, and other proteins, forms a protective mRNP in SGs. The

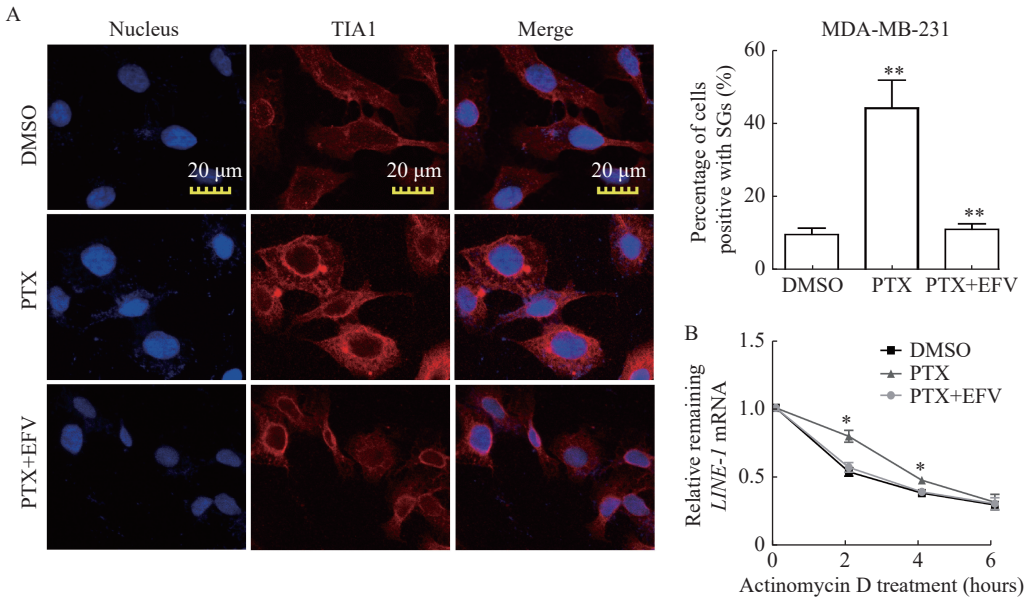

Fig. 6 **EFV reduced the stability of *LINE-1* mRNA by inhibiting the formation of SGs.** A: MDA-MB-231 cells were treated with DMSO (vehicle control) or 100 nmol/L PTX with or without 45 μmol/L EFV for 24 hours, followed by fixation for immunofluorescence. Representative images of the formed SGs (left panel). The percentages of SG-positive cells were calculated (right panel). B: Cells were treated with DMSO, PTX (100 nmol/L), or a combination of PTX and EFV for 24 hours, followed by treatment with 2 μmol/L actinomycin D for 2, 4, or 6 hours to inhibit transcription. qRT-PCR was used to analyze the decay of mRNAs (normalized to *RPLP0* mRNA levels). Mean values±SD (error bars) was shown for three independent experiments. Statistics were performed by *t*-test. $^{*}P<0.05$, $^{**}P<0.01$. PTX: paclitaxel; EFV: efavirenz; SGs: stress granules; DMSO: dimethyl sulfoxide.

recruitment of *LINE-1* mRNA into SGs may increase its recognition by other RNA stabilizer proteins that can form protective mRNPs in SGs. Regardless of the explanation, our results highlighted that SGs can maintain *LINE-1* mRNA stability during chemotherapy drug stress.

A second implication is that SGs induced by chemotherapeutic drugs contribute to in breast cancer cell drug resistance. Although some chemotherapeutics, such as sorafenib, can induce the production of SGs in cancer cells, our finding that the first-line breast cancer chemotherapeutic, PTX, can induce SGs in TNBCs has not been previously reported. Our study proved that PTX can induce the production of SGs in TNBC cells (***Fig. 3A***, ***Supplementary Fig. 2B***, available online). The formation of SGs is usually triggered by phosphorylation of the translation initiation factor eIF2α[14]. The enzymes that phosphorylate eIF2α differ depending on the chemotherapy agent. For example, sorafenib functions by PERK-mediated phosphorylation, while bortezomib functions by HRI-mediated phosphorylation, of eIF2α to induce SGs[39].

Changes in other translation complexes also trigger the formation of SGs. For example, hydrogen peroxide inhibits translation initiation by disrupting the interaction between eIF4E and eIF4G, thereby initiating the assembly of SGs[15]. Similarly, melamine A interferes with translation initiation by blocking the eIF4A helicase required by the ribosome to start the assembly of SGs[40]. In our study, we did not find significantly changed phosphorylation levels for eIF2α after the cells were exposed to 100 nmol/L PTX at different time points (data not shown). This suggested that PTX may induce the assembly of SGs by affecting other translation components, and further experimental investigation is needed.

Consistent with studies on other cancers[17–18], we also confirmed that the SGs induced by chemotherapeutic agents also promoted drug resistance in TNBC cells. We found that interference TIA1 reduced the formation of SGs and improved the sensitivity of drug-resistant breast cancer cells to PTX (***Fig. 3B*** and ***D***). In particular, we found that the PTX-induced SGs promoted breast cancer resistance by improving the stability and level of *LINE-1* mRNA. Two possible mechanisms might explain how the SG stabilization of LINE-1 promoted drug resistance. One is that *LINE-1* mRNA was recruited into the SGs to provide transient protection. The stabilized mRNA then was exchanged quickly and translated to promote cell survival after the relief of the drug stress. This was supported by the significantly increased LINE-1 protein level after PTX was removed 8 hours later (data not shown). Chemotherapy is a cyclical administration process, which means that the stress is switched on and off

periodically, so this would cause a gradual accumulation of LINE-1 levels. The elevated LINE-1 protein level in MDA-MB-231R cells (***Fig. 1A***), which were established by mimic clinical chemotherapy, supports this hypothesis. Another possible mechanism is that the LINE-1 RNA may help to maintain SG structures by forming RNA guanine quadruplexes (G-quadruplexes). The mammalian LINE-1 3 ′UTR contains conserved guanine-rich sequences that can fold into G-quadruplexes[41]. In addition to protein-protein and protein-RNA interactions, RNA-RNA interactions are also an important components of SG structures. G-quadruplexes are noncanonical secondary structures formed by guanine-rich nucleic acids and stabilized by the stacking of guanine tetrads held together by Hoogsteen base pairing. Guanosine can transform into hydrogel-like state structures[42–43] that aid in SG condensation[44]. SG proteins like YB1, hnRNPA1 and FUS have been reported to interact with G quadruplexes[45]. LINE-1 RNA was transported to SGs under stress (***Fig. 4A***), and high concentrations of RNA would promote their self-stacking into G-quadruplexes by the guanine-rich 3 ′UTR. This structure not only stabilizes itself but it also helps to maintain the SG structure. However, this is just a reasonable hypothesis and still needs further experiments for verification.

A third implication is that EFV can also inhibit the formation of drug-induced SGs. EFV is a non-nucleoside reverse transcriptase inhibitor that functions by directly binding to reverse transcriptase to inhibit its activity. In addition to being used as an inhibitor of HIV-1 encoding RT, it can also effectively inhibit the RT activity of the LINE-1 ORF2p, thereby inhibiting the transposition of LINE-1 and reducing the proliferation of cancer cells[46–47]. *In vivo* experiments and clinical studies have shown that EFV can reduce the growth of tumor cells[25,48]; however, whether it also enhances the effect of chemotherapeutics and reverses drug resistance is not clear. Our results proved that EFV can significantly enhance the effects of multiple chemotherapeutics, including paclitaxel, cisplatin, and epirubicin (***Fig. 1D***), which compensates the deficiencies of previous studies. The combination of EFV and chemotherapeutics also appears to be a promising strategy for reversing the cell resistance phenotype. In addition, our research also revealed a new mechanism by which EFV may inhibit LINE-1 levels and exert an anti-tumor effect, as EFV can reduce the mRNA stability of LINE-1 by inhibiting the SGs induced by chemotherapeutics (***Fig. 6A*** and ***B***).

The possible mechanism used by EFV to inhibit the formation of SGs is autophagy induction. SGs are disassembled by translation recovery, chaperone-mediated disaggregation, and autophagy[14]. Autophagy eliminates SGs through a process called granulophagy, which is mainly mediated by the ATPase ACP[49]. EFV can induce autophagy under certain experimental conditions and can show time and concentration dependence. For example, Bellisai *et al* found that 20 μmol/L EFV induced autophagy in the PC3 prostate cancer cell line after 96 hours of treatments, but it did not induce autophagy in PNT2 normal prostate epithelial cells[50]. Phillip *et al* found that 5 μmol/L EFV treatment for 4 hours and 24 hours induced autophagy in SH-SY5Y neuroblastoma cells[51], while Apostolova *et al* found that after 24 hours treatment with 10 to 50 μmol/L EFV induced autophagy in a concentration-dependent manner in Hep3B the human liver cancer cell line[52]. The NDP52 and p62 autophagy receptors can mediate the degradation of LINE-1 RNA, and this may further support the possibility that EFV can inhibit SG stabilization of LINE-1 by inducing autophagy[53]. Whether EFV can inhibit SGs by inducing autophagy in breast cancer cells, and whether this inhibitory effect has tissue and cell specificity, is worth further study.

The final implication is that SGs may also regulate LINE-1 in the tumorigenesis and cancer progression. Tumor cells are well known to undergo challenges like hypoxia, hypertonicity, and nutritional deficiencies due to high replication rates[54]. SGs formation is helpful for the adaption and survival of cancer cells in these unfavorable environments[40,55]. We found that *LINE-1* mRNA was stabilized by the SGs induced by chemotherapy agent PTX. This mechanism may also be applicable in SGs triggered by hypoxia, hypertonicity, and nutritional deficiencies during tumor initiation and progression. Further investigation and verification of the relationship between LINE-1 and SGs in different tumor stages or subtypes would be meaningful for understanding the function of LINE-1 and the pathology of cancers. The role of SGs in LINE-1 post-transcriptional regulation in different cancers and contexts is also worthy of attention.

In conclusion, our results highlighted a new function for SGs in the post-transitional regulation of *LINE-1* mRNA that could be an important survival mechanism for cancer cells exposed to chemotherapy drugs. The findings also enhance our understanding of the mechanisms of chemotherapy resistance and provide evidence of developing new chemotherapeutic

strategies. We believe that the crosstalk between LINE-1 and SGs represents a promising and understudied field.

Acknowledgments

This work was supported by the National Natural Science Foundation of China (Grant No. 82072580 and No. 81572789). We thank all of our colleagues in the laboratory for their assistance during the progression of this study.

References

[1] Foulkes WD, Smith IE, Reis-Filho JS. Triple-negative breast cancer[J]. *N Engl J Med,* 2010, 363(20): 1938–1948.

[2] Liedtke C, Mazouni C, Hess KR, et al. Response to neoadjuvant therapy and long-term survival in patients with triple-negative breast cancer[J]. *J Clin Oncol,* 2008, 26(8): 1275–1281.

[3] Burns KH. Transposable elements in cancer[J]. *Nat Rev Cancer,* 2017, 17(7): 415–424.

[4] Kazazian HH Jr, Goodier JL. LINE drive: retrotransposition and genome instability[J]. *Cell,* 2002, 110(3): 277–280.

[5] Schwertz H, Rowley JW, Schumann GG, et al. Endogenous LINE-1 (long interspersed nuclear element-1) reverse transcriptase activity in platelets controls translational events through RNA-DNA hybrids[J]. *Arterioscler Thromb Vasc Biol,* 2018, 38(4): 801–815.

[6] Dueva R, Akopyan K, Pederiva C, et al. Neutralization of the positive charges on histone tails by RNA promotes an open chromatin structure[J]. *Cell Chem Biol,* 2019, 26(10): 1436–1449.e5.

[7] Cruickshanks HA, Vafadar-Isfahani N, Dunican DS, et al. Expression of a large LINE-1-driven antisense RNA is linked to epigenetic silencing of the metastasis suppressor gene *TFPI-2* in cancer[J]. *Nucleic Acids Res,* 2013, 41(14): 6857–6869.

[8] Lavasanifar A, Sharp CN, Korte EA, et al. Long interspersed nuclear element-1 mobilization as a target in cancer diagnostics, prognostics and therapeutics[J]. *Clin Chim Acta,* 2019, 493: 52–62.

[9] Yang Q, Feng F, Zhang F, et al. LINE-1 ORF-1p functions as a novel HGF/ETS-1 signaling pathway co-activator and promotes the growth of MDA-MB-231 cell[J]. *Cell Signal,* 2013, 25(12): 2652–2660.

[10] Feng F, Lu Y, Zhang F, et al. Long interspersed nuclear element ORF-1 protein promotes proliferation and resistance to chemotherapy in hepatocellular carcinoma[J]. *World J Gastroenterol,* 2013, 19(7): 1068–1078.

[11] Farkash EA, Kao GD, Horman SR, et al. Gamma radiation increases endonuclease-dependent L1 retrotransposition in a cultured cell assay[J]. *Nucleic Acids Res,* 2006, 34(4): 1196–1204.

[12] Okudaira N, Okamura T, Tamura M, et al. Long interspersed element-1 is differentially regulated by food-borne carcinogens *via* the aryl hydrocarbon receptor[J]. *Oncogene,* 2013, 32(41): 4903–4912.

[13] Guler GD, Tindell CA, Pitti R, et al. Repression of stress-induced LINE-1 expression protects cancer cell subpopulations from lethal drug exposure[J]. *Cancer Cell,* 2017, 32(2): 221–237.e13.

[14] Mahboubi H, Stochaj U. Cytoplasmic stress granules: dynamic modulators of cell signaling and disease[J]. *Biochim Biophys Acta Mol Basis Dis,* 2017, 1863(4): 884–895.

[15] Fujimura K, Sasaki AT, Anderson P. Selenite targets eIF4E-binding protein-1 to inhibit translation initiation and induce the assembly of non-canonical stress granules[J]. *Nucleic Acids Res,* 2012, 40(16): 8099–8110.

[16] Liu W, Huang CY, Lu IC, et al. Inhibition of glioma growth by minocycline is mediated through endoplasmic reticulum stress-induced apoptosis and autophagic cell death[J]. *Neuro Oncol,* 2013, 15(9): 1127–1141.

[17] Vilas-Boas FDAS, da Silva AM, de Sousa LP, et al. Impairment of stress granule assembly *via* inhibition of the eIF2alpha phosphorylation sensitizes glioma cells to chemotherapeutic agents[J]. *J Neurooncol,* 2016, 127(2): 253–260.

[18] Arimoto K, Fukuda H, Imajoh-Ohmi S, et al. Formation of stress granules inhibits apoptosis by suppressing stress-responsive MAPK pathways[J]. *Nat Cell Biol,* 2008, 10(11): 1324–1332.

[19] Thedieck K, Holzwarth B, Prentzell MT, et al. Inhibition of mTORC1 by astrin and stress granules prevents apoptosis in cancer cells[J]. *Cell,* 2013, 154(4): 859–874.

[20] Gareau C, Fournier MJ, Filion C, et al. $p21^{WAF1/CIP1}$ upregulation through the stress granule-associated protein CUGBP1 confers resistance to bortezomib-mediated apoptosis[J]. *PLoS One,* 2011, 6(5): e20254.

[21] Doucet AJ, Hulme AE, Sahinovic E, et al. Characterization of LINE-1 ribonucleoprotein particles[J]. *PLoS Genet,* 2010, 6(10): e1001150.

[22] Khong A, Matheny T, Jain S, et al. The stress granule transcriptome reveals principles of mRNA accumulation in stress granules[J]. *Mol Cell,* 2017, 68(4): 808–820.e5.

[23] Ying W, Wang S, Shi J, et al. ER-/ER+ breast cancer cell lines exhibited different resistance to paclitaxel through pulse selection[J]. *Med Oncol,* 2012, 29(2): 495–502.

[24] Bojang P Jr, Roberts RA, Anderton MJ, et al. Reprogramming of the HepG2 genome by long interspersed nuclear element-1[J]. *Mol Oncol,* 2013, 7(4): 812–825.

[25] Sciamanna I, Landriscina M, Pittoggi C, et al. Inhibition of endogenous reverse transcriptase antagonizes human tumor growth[J]. *Oncogene,* 2005, 24(24): 3923–3931.

[26] Győrffy B, Lanczky A, Eklund AC, et al. An online survival analysis tool to rapidly assess the effect of 22, 277 genes on breast cancer prognosis using microarray data of 1, 809 patients[J]. *Breast Cancer Res Treat,* 2010, 123(3): 725–731.

[27] Agostini F, Zanzoni A, Klus P, et al. *cat*RAPID *omics*: a web

server for large-scale prediction of protein-RNA interactions[J]. *Bioinformatics,* 2013, 29(22): 2928–2930.

[28] Muppirala UK, Honavar VG, Dobbs D. Predicting RNA-protein interactions using only sequence information[J]. *BMC Bioinformatics,* 2011, 12: 489.

[29] Kale SP, Moore L, Deininger PL, et al. Heavy metals stimulate human LINE-1 retrotransposition[J]. *Int J Environ Res Public Health,* 2005, 2(1): 14–23.

[30] Teneng I, Stribinskis V, Ramos KS. Context-specific regulation of *LINE-1*[J]. *Genes Cells,* 2007, 12(10): 1101–1110.

[31] Whongsiri P, Pimratana C, Wijitsettakul U, et al. LINE-1 ORF1 protein is Up-regulated by reactive oxygen species and associated with bladder urothelial carcinoma progression[J]. *Cancer Genomics Proteomics,* 2018, 15(2): 143–151.

[32] Lim J, Ha M, Chang H, et al. Uridylation by TUT4 and TUT7 marks mRNA for degradation[J]. *Cell,* 2014, 159(6): 1365–1376.

[33] Hamdorf M, Idica A, Zisoulis DG, et al. miR-128 represses L1 retrotransposition by binding directly to L1 RNA[J]. *Nat Struct Mol Biol,* 2015, 22(10): 824–831.

[34] Fung L, Guzman H, Sevrioukov E, et al. miR-128 restriction of LINE-1 (L1) retrotransposition is dependent on targeting hnRNPA1 mRNA[J]. *Int J Mol Sci,* 2019, 20(8): 1955.

[35] Kawakami A, Tian Q, Duan X, et al. Identification and functional characterization of a TIA-1-related nucleolysin[J]. *Proc Natl Acad Sci USA,* 1992, 89(18): 8681–8685.

[36] Meyer C, Garzia A, Mazzola M, et al. The TIA1 RNA-binding protein family regulates EIF2AK2-mediated stress response and cell cycle progression[J]. *Mol Cell,* 2018, 69(4): 622–635.e6.

[37] Bley N, Lederer M, Pfalz B, et al. Stress granules are dispensable for mRNA stabilization during cellular stress[J]. *Nucleic Acids Res,* 2015, 43(4): e26.

[38] Goodier JL, Zhang L, Vetter MR, et al. LINE-1 ORF1 protein localizes in stress granules with other RNA-binding proteins, including components of RNA interference RNA-induced silencing complex[J]. *Mol Cell Biol,* 2007, 27(18): 6469–6483.

[39] Song MS, Grabocka E. Stress granules in cancer[M]// Pedersen SHF. Reviews of physiology, biochemistry and pharmacology. Berlin Heidelberg: Springer, 2020: 1–28.

[40] Anderson P, Kedersha N, Ivanov P. Stress granules, P-bodies and cancer[J]. *Biochim Biophys Acta,* 2015, 1849(7): 861–870.

[41] Sahakyan AB, Murat P, Mayer C, et al. G-quadruplex structures within the 3′UTR of LINE-1 elements stimulate retrotransposition[J]. *Nat Struct Mol Biol,* 2017, 24(3): 243–247.

[42] Gellert M, Lipsett MN, Davies DR. Helix formation by guanylic acid[J]. *Proc Natl Acad Sci U S A,* 1962, 48(12): 2013–2018.

[43] Kato M, Han TW, Xie S, et al. Cell-free formation of RNA granules: low complexity sequence domains form dynamic fibers within hydrogels[J]. *Cell,* 2012, 149(4): 753–767.

[44] Van Treeck B, Protter DSW, Matheny T, et al. RNA self-assembly contributes to stress granule formation and defining the stress granule transcriptome[J]. *Proc Natl Acad Sci U S A,* 2018, 115(11): 2734–2739.

[45] Ivanov P, O'Day E, Emara MM, et al. G-quadruplex structures contribute to the neuroprotective effects of angiogenin-induced tRNA fragments[J]. *Proc Natl Acad Sci U S A,* 2014, 111(51): 18201–18206.

[46] Dai L, Huang Q, Boeke JD. Effect of reverse transcriptase inhibitors on LINE-1 and Ty1 reverse transcriptase activities and on LINE-1 retrotransposition[J]. *BMC Biochem,* 2011, 12: 18.

[47] Hecht M, Erber S, Harrer T, et al. Efavirenz has the highest anti-proliferative effect of non-nucleoside reverse transcriptase inhibitors against pancreatic cancer cells[J]. *PLoS One,* 2015, 10(6): e0130277.

[48] Houédé N, Pulido M, Mourey L, et al. A phase II trial evaluating the efficacy and safety of efavirenz in metastatic castration-resistant prostate cancer[J]. *Oncologist,* 2014, 19(12): 1227–1228.

[49] Buchan JR, Kolaitis RM, Taylor JP, et al. Eukaryotic stress granules are cleared by autophagy and Cdc48/VCP function[J]. *Cell,* 2013, 153(7): 1461–1474.

[50] Bellisai C, Sciamanna I, Rovella P, et al. Reverse transcriptase inhibitors promote the remodelling of nuclear architecture and induce autophagy in prostate cancer cells[J]. *Cancer Lett,* 2020, 478: 133–145.

[51] Purnell PR, Fox HS. Efavirenz induces neuronal autophagy and mitochondrial alterations[J]. *J Pharmacol Exp Ther,* 2014, 351(2): 250–258.

[52] Apostolova N, Gomez-Sucerquia LJ, Gortat A, et al. Compromising mitochondrial function with the antiretroviral drug efavirenz induces cell survival-promoting autophagy[J]. *Hepatology,* 2011, 54(3): 1009–1019.

[53] Guo H, Chitiprolu M, Gagnon D, et al. Autophagy supports genomic stability by degrading retrotransposon RNA[J]. *Nat Commun,* 2014, 5: 5276.

[54] Gorrini C, Harris IS, Mak TW. Modulation of oxidative stress as an anticancer strategy[J]. *Nat Rev Drug Discov,* 2013, 12(12): 931–947.

[55] Protter DSW, Parker R. Principles and properties of stress granules[J]. *Trends Cell Biol,* 2016, 26(9): 668–679.